Modelling and Handling Quality Assessment of the Flying-V Aircraft

van Overeem, S.; Wang, Xuerui; van Kampen, E.

DOI
10.2514/6.2022-1429

Publication date
2022

Document Version
Final published version

Published in
AIAA SCITECH 2022 Forum

AIAA SciTech Forum
January 3-7, 2022, San Diego, CA & Virtual
AIAA SCITECH 2022 Forum

10.2514/6.2022-1429

Modelling and Handling Quality Assessment of the Flying-V Aircraft

Simon van Overeem* and Xuerui Wang† and Erik-Jan van Kampen‡
Delft University of Technology, The Netherlands, 2629 HS Delft

Considerable growth in the number of passengers and cargo transported by air is predicted. Besides that, aircraft noise and climate impact become increasingly important factors in aircraft design. These existing challenges in aviation boost interest in the design of innovative aircraft configurations. One of these configurations is a V-shaped flying wing named the Flying-V. This work aims at developing a flight dynamic simulation model of the Flying-V based on aerodynamic data obtained from the Vortex Lattice Method and wind tunnel experiments. The simulation model is used to assess the stability and handling qualities for certification and qualification purposes. Prior work has shown an assessment of the stability and handling qualities based on a linear aerodynamic model. However, to capture the longitudinal undesired behaviour of the Flying-V it is necessary to use a nonlinear aerodynamic model. Therefore, this paper illustrates how a flight dynamic simulation model, based on combined aerodynamic data from the Vortex Lattice Method and wind tunnel experiments, is used for certification and qualification purposes. The stability and handling qualities are assessed by analysing the aircraft dynamic modes and analysing nonlinear system handling qualities based on linearisation for both the cruise and approach condition.

I. Introduction

Over the last five decades, the majority of commercial aircraft consisted of the traditional tube-and-wing configuration. This conventional design has obtained significant efficiency gains of 100% over the years [1]. However, the Airbus A350 and Boeing 787 represent an asymptote regarding aircraft efficiency. Besides that, considerable growth in the number of passengers and cargo transported by air is predicted [2]. Furthermore, since the reduction of aircraft noise and environmental impact become more important factors in aircraft design, there is a necessity for a solution that is able to boost the efficiency for the increasing number of passengers and cargo, while reducing noise and environmental impact [3]. One course of action to overcome the existing challenges in aviation is the design of an innovative aircraft configuration. One of the most promising aircraft configurations for future operations is the flying wing in all its different settings such as the Blended-Wing-Body (BWB), C-Wing, and Tail-less aircraft. Flying wings have the potential to significantly increase efficiency, resulting in less pollution, and reduce noise levels during landing and take-off [3].

The Flying-V is a specific type of flying wing that is tailless, V-shaped, and consists of two cylindrical pressurised cabins located in the leading edge of the wing. The design of a Flying-V aircraft concept contains several benefits compared to conventional tube-and-wing aircraft. The main advantage of this type of aircraft is the reduction of wetted area and frictional drag since one structure integrates the structural function of accommodating payload and aerodynamic function of providing lift [4]. Furthermore, this type of aircraft suffers less from interference drag due to the smooth shape of the configuration. Additionally, the reduced wetted area per unit of useful volume results in a reduction of the zero-lift drag [5]. Therefore, this type of aircraft can achieve a higher lift-to-drag ratio compared to conventional aircraft and hence has a reduced fuel burn and takeoff weight [6, 7]. Research on the aerodynamic advantages of the Flying-V presents that the aircraft can have aerodynamic efficiency gains ranging from 10% to 25% compared to conventional tube-and-wing aircraft of similar size and weight while reducing the noise level due to the location of the engines on top of the wing [2, 7]. The preliminary design of the Flying-V is shown in Fig. 1.

Currently, the two main Flying-V design challenges are centred on modelling and assessment of the stability and handling qualities of this novel aircraft design for certification and qualification purposes. Previous research is conducted on the stability and handling qualities of the full-size aircraft by designing a six degrees-of-freedom flight dynamic toolbox using aerodynamic coefficients obtained from the Vortex Lattice Method and inertia estimations obtained

*Graduate Student, Faculty of Aerospace Engineering at Delft University of Technology, s.vanovereem@student.tudelft.nl
†Assistant Professor, Faculty of Aerospace Engineering at Delft University of Technology, X.Wang-6@tudelft.nl, AIAA member
‡Assistant Professor, Faculty of Aerospace Engineering at Delft University of Technology, E.vanKampen@tudelft.nl

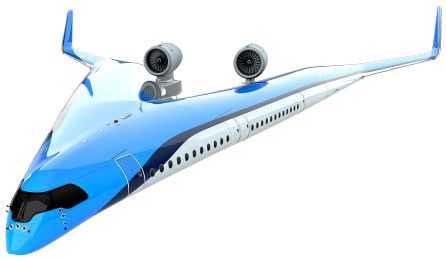

Fig. 1 The Flying-V developed by Delft University of Technology.*

using a lumped mass method. A stability and handling quality assessment is performed using military standards and requirements obtained from the European Aviation Safety Agency (EASA). The main limitation of previous research is the use of linearised aerodynamic data, meaning that the aerodynamic model is not able to accurately describe the corners of the flight envelope and that deviation from the linearisation points results in inaccurate estimations. Previous research concludes that the Dutch roll mode is unstable and that the lateral-directional controllability of the aircraft is limited in the case of One Engine Inoperative (OEI) at low speeds [8]. The unstable Dutch roll behaviour obtained from previous research was confirmed during a flight test with a small scale model of the aircraft* and is also in coherence with previous research on the undesirable lateral-directional behaviour of flying wings [9, 10]. In preparation for this flight test, wind tunnel experiments have been performed on a half-span small scale model of the Flying-V. These experiments focus on the longitudinal flight characteristics of the Flying-V small scale model for which the centre of gravity range is determined (1.32 m - 1.40 m from the nose of the aircraft) to guarantee trimmability of the aircraft at approach speeds and high angles of attack. Besides that, the Flying-V shows longitudinal unstable behaviour in case the angle of attack is larger than 20° [11, 12]. This longitudinal unstable behaviour is also captured in an aerodynamic model obtained from wind tunnel experiments to perform aerodynamic model identification of the Flying-V half-span small scale model. Due to limitations of the experiments, the aerodynamic model obtained from these experiments only considers the longitudinal static aerodynamic coefficients [13].

This study consists of two contributions to research related to the Flying-V aircraft. First of all, this study integrates the aerodynamic models that are obtained from the Vortex Lattice Method and wind tunnel experiments into a rigid six degrees-of-freedom flight dynamic simulation model that is able to capture the undesired behaviour of the Flying-V revealed by previous research, such as the unstable Dutch roll mode and longitudinal unstable behaviour. Secondly, this research aims to assess the most essential stability and handling qualities of the Flying-V during cruise and approach conditions for several centre of gravity locations using the flight dynamic simulation model.

The rest of this paper is structured as follows. Section II elaborates on the essential stability and handling qualities assessed using the flight dynamic simulation model. Besides that, the flight dynamic simulation model design is discussed including combining the aerodynamic models obtained from the Vortex Lattice Method and wind tunnel experiments. In section III, the results of the assessment of the essential stability and handling qualities of the Flying-V are shown. Finally, conclusions are discussed in section IV and recommendations for further research are given in section V.

II. Methodology

In this section, the methodology to assess the stability and handling qualities of the Flying-V is discussed in section II.A. After that, section II.B elaborates on the design of the flight dynamic simulation model.

A. Stability and Handling Quality Assessment

In this section, the key stability and handling quality requirements for certification and qualification purposes are discussed. In section II.A.1, the trimmability of the Flying-V is discussed. After that, section II.A.2 elaborates on the responses of the eigenmodes. Finally, section II.A.3 discusses the handling qualities.

*https://www.tudelft.nl/en/2020/tu-delft/successful-maiden-flight-for-the-tu-delft-flying-v

1. Trim

The requirements for aircraft trim are obtained from EASA CS25.161 (Trim) [14]. Trim requirements can be subdivided into longitudinal and lateral-directional requirements. These requirements are discussed below for the cruise phase and approach phase.

Longitudinal Trim

During the approach phase, the aircraft must have the ability to be trimmed within the normal range of approach speeds with power settings corresponding to a glidepath angle of 3° for the most unfavourable combination of centre of gravity position and weight approved for landing [14].

During the cruise phase, the aircraft must have the ability to be trimmed at any airspeed ranging between 1.3 times the stall speed and the maximum operating limit speed with the landing gear and wing-flaps retracted [14].

Based on the availability of aerodynamic data, the longitudinal trimmability of the aircraft is assessed for Ma = 0.2 during approach and Ma = 0.85 during cruise. Furthermore, the most forward and aft centre of gravity locations are considered (29.372 m and 31.714 m from the nose respectively). It is expected that the longitudinal trimmability of the aircraft is mainly demanding for low airspeeds [15]. Due to limited research on the aerodynamic effects of extending the landing gear of the Flying-V, an approach phase with landing gear retracted is considered.

Lateral-Directional Trim

The aircraft must have the ability to maintain lateral-directional trim with the most adverse lateral displacement of the centre of gravity at any airspeed ranging between 1.3 times the stall speed and the maximum operating limit speed [14]. During the analysis of the Flying-V, it is assumed that the centre of gravity is located in the plane of symmetry of the aircraft. Therefore, lateral-directional trim is not considered for this research.

2. Modes Response

Because civil aviation authorities do not provide quantifiable requirements for the longitudinal and lateral-directional modes of an aircraft, it is decided to use military (quantifiable) requirements to assess the dynamic modes of the Flying-V [16]. To use these military standards, it is necessary to identify the aircraft class and prevailing flight conditions. According to these standards, aircraft can be divided into several classes namely: Class I (small light aircraft), Class II (medium weight, low to medium manoeuvrability aircraft), Class III (large, heavy, low to medium manoeuvrability aircraft), and Class IV (high manoeuvrability aircraft) [17, 18]. Besides that, flight phases can be divided into several categories. Category A consists of non-terminal flight phases that require rapid manoeuvring, precision tracking, or precise flight path control such as ground attacks, aerobatics, and close formation flight. Category B consists of non-terminal flight phases that require gradual manoeuvring, less precise tracking and accurate flight path control such as climb, cruise, and loiter. Category C consists of terminal flight phases that require gradual manoeuvring and precision flight path control such as takeoff, approach, and landing [17, 18]. Based on these classes and flight phases the Flying-V can be considered a Class III aircraft with prevailing flight phases in Category B and Category C.

To identify the ability of the aircraft to complete the mission for which it is designed, three levels of flying qualities can be defined that indicate the severity of the pilot workload during the execution of a specific flight phase. In case the flying qualities of an aircraft are rated Level 1, the flying qualities are adequate for the mission flight phase. Furthermore, Level 2 flying qualities correspond to adequacy for the mission flight phase, but with an increase in pilot workload and, or, degradation in mission effectiveness. Finally, Level 3 flying qualities describe degraded flying qualities, but such that the aircraft can be controlled with inadequate mission effectiveness and high pilot workload [17, 18]. To assess the modes it is first necessary to linearise the equations of motion such that specific parameters such as the damping ratio, natural frequency, and characteristic time constants can be determined. These parameters are used to compare the characteristics of the Flying-V with military standards. Consequently, it is possible to give a quantifiable measure for the flying qualities of the aircraft. The specific modes are discussed below.

Short-Period Mode

The short-period motion is an oscillating pitch rate response. This motion is fast and is the transient response of an elevator input. Therefore, to have a sufficient tracking of a reference signal, the short-period must be well damped to reach a steady state pitch condition quickly [19]. To assess the short period mode, it is necessary to determine the damping ratio of this mode and compare it with military standards [17, 18].

Phugoid Mode

The phugoid is a slow pitch angle response. During a phugoid motion, the aircraft follows a sinusoidal path, while interchanging potential energy with kinetic energy [19]. In general, the phugoid dynamics are considered acceptable in case the mode is stable and the damping ratio adheres to the limits set by military standards [17, 18].

Dutch Roll Mode

The Dutch roll is a yawing and simultaneously rolling motion that originates from a sideslip deviation that induces a yawing motion. Aerodynamic coupling results in the rolling of the aircraft. The vertical tail surface of a conventional aircraft has the largest contribution in dampening the motion [19]. The Dutch roll mode can be considered as a short-period mode in the lateral direction and has therefore an important influence on lateral-directional handling qualities. It is therefore assessed using the damping ratio and frequency of the mode [17, 18].

Aperiodic Roll Mode

The aperiodic roll mode represents the quick response of the roll rate to a roll control input. In case the roll control input is removed, the roll rate should return to zero [19]. The aperiodic roll mode can be assessed by determining the characteristic time constant (T_r) and comparing it with military standards [17, 18].

Spiral Mode

The spiral mode is a slowly developing turning flight when the aircraft spirals down. In case this motion is stable, the aircraft returns to wings level flight after a roll input (either a roll disturbance or pilot input) is applied to the aircraft. In case this motion is unstable, the roll angle slowly increases [19]. In case the spiral mode is stable, it is always acceptable irrespective of its time constant. Because this mode generally involves slow dynamic behaviour, it is not a very critical mode, unless the mode is very unstable. For this reason, the minimum acceptable degrees of instability are quantified in terms of the spiral time constant (T_s), which is a function of the time to double bank angle (T_2) during an uncontrolled departure from straight and level flight [17, 18].

3. Handling Qualities

The handling qualities of an aircraft are considered as a description of the adequacy of the short term dynamic response to controls during the execution of a flight task [17]. The main focus of the handling qualities discussed in this research involves quantitative handling qualities as these quantitative methods do not require pilot-in-the-loop experiments. However, it needs to be noted that potential future pilot-in-the-loop experiments are taken into account while analysing the handling qualities. The handling quality assessed for this research consist of the Control Anticipation Parameter (CAP). This is a measure of manoeuvrability of the aircraft. In case the CAP is too high, the aircraft's response is faster than would be expected by the pilot resulting in understeering. On the other hand, in case the CAP is too low, the aircraft's response is sluggish, which results in oversteering [8].

B. Flight Dynamic Simulation Model Design

In this section, the simulation model design is discussed. In section II.B.1 the frames of reference used during the simulation are discussed. After that, section II.B.2 elaborates on the dynamic and kinematic equations. Furthermore, in section II.B.3 the aerodynamic model is discussed. Also, section II.B.4 shows the methodology for verification and validation of the simulation model. Finally, section II.B.5 elaborates on the assumptions and limitations of the simulation model.

1. Frames of Reference

Before the stability and handling qualities of the aircraft can be analysed, it is necessary to define two coordinate frames. First of all, it is necessary to define the vehicle-carried normal Earth reference frame ($\mathcal{E}$-frame). This frame has the $X_{\mathcal{E}}$-axis directed to the north and the $Y_{\mathcal{E}}$-axis directed 90 degrees to the right of the $X_{\mathcal{E}}$-axis (to the east). In case it is assumed that the Earth is spherical, the $Z_{\mathcal{E}}$-axis is pointed in the direction of the centre of the Earth. However, for this analysis it is assumed that the Earth is a flat plate. Therefore, the $Z_{\mathcal{E}}$-axis points downwards, and the vehicle-carried normal Earth reference frame is an inertial frame. Besides that, the body fixed reference frame can be defined (the $\mathcal{B}$-frame). For this frame, the $X_{\mathcal{B}}$-axis is located in the plane of symmetry and points forward. The $Z_{\mathcal{B}}$-axis is also located in the symmetry plane and points downwards. Finally, the $Y_{\mathcal{B}}$-axis completes the right-handed coordinate system

and points perpendicular to both the $X_{\mathcal{B}}$-axis and the $Z_{\mathcal{B}}$-axis. The two frames can be observed in Fig. 2.

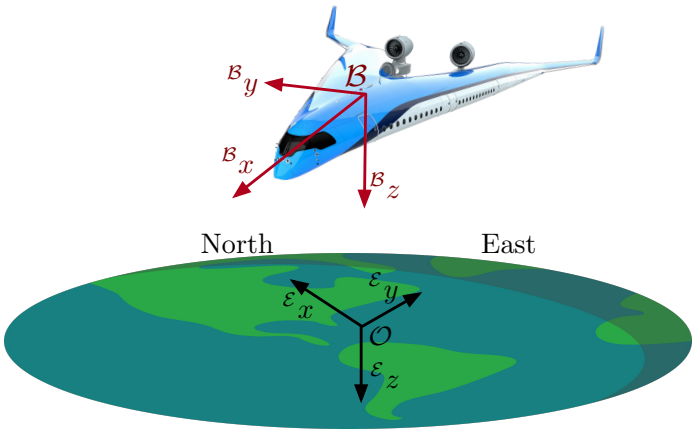

Fig. 2 Frames of reference.

2. Dynamics and Kinematics

After derivation of the equations of motion it is possible to obtain the dynamic equations as shown in Eq. (1). The states of this system consist of the velocity in body-frame components (${}^{\mathcal{B}}\boldsymbol{v}$) and the angular velocity of the body-frame with respect to the Earth-frame in body-frame components (${}^{\mathcal{B}}\boldsymbol{\omega}_{\mathcal{B}/\mathcal{E}}$). Besides that, the angular velocity matrix and inertia matrix are shown (${}^{\mathcal{B}}\Omega_{\mathcal{B}/\mathcal{E}}$ and J respectively). Finally, the force and moments consist of the forces due to gravity (${}^{\mathcal{B}}\boldsymbol{F}_{\text{grav}}$), aerodynamic forces (${}^{\mathcal{B}}\boldsymbol{F}_{\text{aero}}$), the thrust force (${}^{\mathcal{B}}\boldsymbol{F}_{\text{thrust}}$), aerodynamic moments (${}^{\mathcal{B}}\boldsymbol{M}_{\text{aero}}$), moments due to thrust (${}^{\mathcal{B}}\boldsymbol{M}_{\text{thrust}}$), and moments due to a shift in the centre of gravity (${}^{\mathcal{B}}\boldsymbol{M}_{\text{cg}}$). The moments induced by the centre of gravity shift can be obtained using Eq. (2) [20]. This equation shows that the moment due to a centre of gravity shift can be obtained by first subtracting the centre of gravity position ($\boldsymbol{p}_{\text{cg}}$) from the reference position around which the aerodynamic forces and moments are calculated ($\boldsymbol{p}_{\text{ref}}$). Consequently, a cross product with the aerodynamic forces results in the moment induced by the centre of gravity shift.

$$\begin{bmatrix} {}^{\mathcal{B}}\dot{\boldsymbol{v}} \\ {}^{\mathcal{B}}\dot{\boldsymbol{\omega}}_{\mathcal{B}/\mathcal{E}} \end{bmatrix} = \begin{bmatrix} -{}^{\mathcal{B}}\Omega_{\mathcal{B}/\mathcal{E}} & 0 \\ 0 & -J^{-1}{}^{\mathcal{B}}\Omega_{\mathcal{B}/\mathcal{E}}J \end{bmatrix} \begin{bmatrix} {}^{\mathcal{B}}\boldsymbol{v} \\ {}^{\mathcal{B}}\boldsymbol{\omega}_{\mathcal{B}/\mathcal{E}} \end{bmatrix} + \begin{bmatrix} \frac{{}^{\mathcal{B}}\boldsymbol{F}_{\text{grav}}}{m} + \frac{{}^{\mathcal{B}}\boldsymbol{F}_{\text{aero}}}{m} + \frac{{}^{\mathcal{B}}\boldsymbol{F}_{\text{thrust}}}{m} \\ J^{-1}\left({}^{\mathcal{B}}\boldsymbol{M}_{\text{aero}} + {}^{\mathcal{B}}\boldsymbol{M}_{\text{thrust}} + {}^{\mathcal{B}}\boldsymbol{M}_{\text{cg}}\right) \end{bmatrix} \tag{1}$$

$$ {}^{\mathcal{B}}\boldsymbol{M}_{\text{cg}} = (\boldsymbol{p}_{\text{ref}} - \boldsymbol{p}_{\text{cg}}) \times {}^{\mathcal{B}}\boldsymbol{F}_{\text{aero}} \tag{2}$$

It is consequently also possible to derive the kinematic equations as can be observed in Eq. (3). In this equation, the roll, pitch, and yaw angles are shown (ϕ, θ, and ψ respectively) together with the roll, pitch, and yaw rates (p, q, and r respectively).

$$\begin{bmatrix} \dot{\phi} \\ \dot{\theta} \\ \dot{\psi} \end{bmatrix} = \begin{bmatrix} 1 & \sin\phi\tan\theta & \cos\phi\tan\theta \\ 0 & \cos\phi & -\sin\phi \\ 0 & \frac{\sin\phi}{\cos\theta} & \frac{\cos\phi}{\cos\theta} \end{bmatrix} \begin{bmatrix} p \\ q \\ r \end{bmatrix}_{\mathcal{B}} \tag{3}$$

To estimate the components of the inertia matrix, the lumped mass method is used. The general idea of this method is to consider the power plant and landing gear as point masses. The rest of the aircraft is divided into lumped masses placed at half chord locations. The lumped masses are divided over point masses equally spaced from the root of the wing to the tip. The spacing is considered to be good enough such that the moment of inertia around each specific point mass is negligible. In the inertia matrix, the coefficients J_{xy} and J_{yz} can be set to zero as the Flying-V is assumed to be a mass-symmetrical vehicle [8].

3. Aerodynamic Model

The undesired behaviour of the Flying-V consists of unstable Dutch roll motion and longitudinal instability for angles of attack larger than 20°. The unstable Dutch roll is obtained from a stability and handling quality analysis using aerodynamic coefficients obtained from the Vortex Lattice Method [8]. Besides that, the longitudinal unstable behaviour of the aircraft was observed during wind tunnel experiments [11, 12] and captured in an aerodynamic model obtained from these wind tunnel experiments [13]. Therefore, this section elaborates on the aerodynamic models obtained from the Vortex Lattice Method and wind tunnel experiments. After that, the methodology used to combine these aerodynamic models into a single aerodynamic model that is able to capture both the unstable Dutch roll and longitudinal instability for angles of attack larger than 20° is discussed.

Vortex Lattice Method

To define the aerodynamic coefficients using the Vortex Lattice Method, the aerodynamic geometry of the aircraft defined in previous work [2] is translated into a panel model that can be used for the aerodynamic estimations. Using this panel method it is possible to compute the lift and induced drag of the aircraft while omitting the thickness and viscosity. The output consists of the aerodynamic coefficients for specific Mach numbers [8]. The aerodynamic model is validated using a comparative analysis of the lift coefficient and pitching moment coefficient obtained from the Vortex Lattice Method with wind tunnel tests performed by [11].

The aerodynamic model obtained from the Vortex Lattice Method also consists of several limitations. First of all, the aerodynamic data is linear, meaning that this model is not able to accurately display the corners of the flight envelope due to nonlinearities. This also means that deviation from the linearisation points results in inaccurate estimations. The model is considered valid for angles of attack ranging between -5° up to 15°. Besides that, frictional drag [21], ground effect, compressibility, and aeroelasticity effects are not taken into account. Also, the atmospheric model does not include wind, turbulence, nor wind shear. Finally, the landing gear and fairing of the Flying-V are not modelled [8]. Due to these limitations, the aerodynamic model obtained from the Vortex Lattice Method cannot be used to model the unstable longitudinal behaviour of the Flying-V. Besides that, the dynamic behaviour of the aircraft may change compared to a real flight due to the components not included into the aerodynamic model.

Wind Tunnel Experiments

To obtain an aerodynamic model from wind tunnel experiments, a 1/22 scaled half-span model of the Flying-V is used (shown in Fig. 3). During these experiments, several independent variables (the angle of attack, wind speed, and elevon deflections) are altered to determine the aerodynamic coefficients (dependent variables). During the identification process, the independent variables are assumed to be not contaminated with noise, while the dependent variables are contaminated with uniformly distributed noise. The measurements are considered accurate enough for angles of attack ranging from -10° up to 30° and airspeeds ranging between 12m/s up to 30m/s. Due to high uncertainties, the lateral force coefficient (C_Y) could not be identified [13].

For the wind tunnel model, it is necessary to take into account that only the half-span clean wing configuration is modelled without landing gear, fairing, nor engines. This results in limited fidelity of this model with respect to the full aircraft configuration. Furthermore, no winglets including rudders are added to the wind tunnel model. For this reason, using this model limits the user to accurately simulate the lateral-directional dynamics of the aircraft. Besides that, outside the fidelity bounds, no measurements were taken during the construction of the aerodynamic model meaning that extrapolating outside this convex hull results in new, unmodeled effects that affect the validity of the model [13]. Due to these limitations, the aerodynamic model obtained from wind tunnel experiments cannot be used to model the lateral-directional dynamics of the Flying-V (including the unstable Dutch roll mode). Besides that, the use of a scaled model that does not include landing gear, fairing, engines, nor winglets affects the dynamic behaviour of the small-scale Flying-V compared to the full-scale aircraft.

Aerodynamic Model Discrepancies

The aerodynamic models obtained from the Vortex Lattice Method (VLM) and wind tunnel experiments (WTE) are different on several aspects that need to be mentioned before the aerodynamic models can be combined into a single aerodynamic model that is able to capture the undesired behaviour obtained from previous research. First of all, the VLM model is a linear model, whereas the WTE model is a nonlinear model. Besides that, the VLM model is based on the full-scale aircraft, whereas the WTE model is based on a small-scale aircraft. Also, the control surface layout of the full-scale aircraft is different from the small-scale aircraft. Namely, the full-scale aircraft consists of an inboard elevon (used for pitch control), an outboard elevon (used for pitch and roll control), and a rudder integrated into the winglet

(used for yaw control). The small-scale aircraft consists of three elevons that can be used for both pitch and roll control, and no winglets nor rudders. The geometrical differences are visible in Fig. 3.

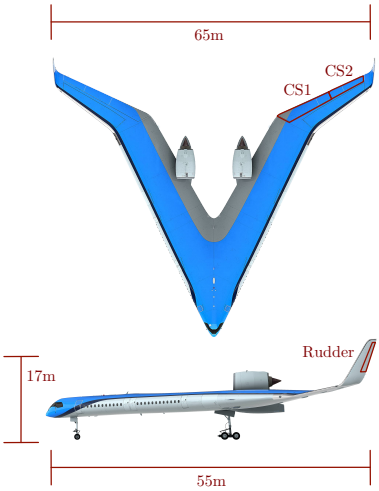

(a) Full-scale Flying-V used for Vortex Lattice Method (landing gear not included for analysis).*

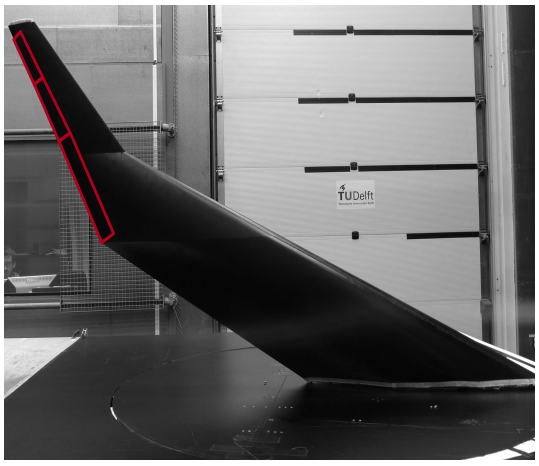

(b) Small-scale Flying-V used for wind tunnel experiments [12].

Fig. 3 Flying-V aircraft used for aerodynamic models.

Aerodynamic Model Design

To design a flight dynamic simulation model that is able to capture the unstable Dutch roll and unstable longitudinal behaviour of the Flying-V it is necessary to combine the aerodynamic model obtained from the Vortex Lattice Method with the aerodynamic model obtained from the wind tunnel experiments. To combine the VLM aerodynamic model and the WTE aerodynamic model, the VLM model is used as the baseline model. This means that the Flying-V model used for this analysis consists of an inboard elevon, outboard elevon, and rudder integrated into the winglet (shown in Fig. 3). After that, elements from the WTE model are implemented into the VLM model, such that the combined model is able to capture the unstable Dutch roll and longitudinal instability obtained from previous research [8, 11, 12]. Therefore, this research combines the coefficients that are relevant for modelling the longitudinal instability. These are the longitudinal force coefficient (C_X), directional force coefficient (C_Z), and pitch moment coefficient (C_M). The remaining coefficients consist of the lateral force coefficient (C_Y), roll moment coefficient (C_L), and yaw moment coefficient (C_N). For these coefficients, the coefficients obtained from the VLM model are used. Besides that, the aerodynamic coefficients are determined for the approach- and cruise condition (Ma = 0.2 and Ma = 0.85 respectively) for angles of attack ranging between $-5°$ and $30°$. Additionally, due to the significant difference in control surface layout between the two models, deflections are kept equal to zero. Essentially, this means that the aerodynamic model combination entails combining the contribution of the angle of attack to the coefficients: C_X, C_Z, and C_M.

Both aerodynamic models operate in different airspeed regimes due to the difference in aircraft size. Therefore it is necessary to scale the airspeed according to Dynamic or Froude scaling. This scaling method can be used for scaled aircraft models that are capable of simulating the relative motions of a larger full-scale aircraft [22]. After scaling the airspeed, it is possible to compare the aerodynamic coefficients for different angles of attack as shown in Fig. 4.

This figure shows that the aerodynamic coefficients of the VLM and WTE are of the same magnitude, but that the VLM model is not able to capture the longitudinal instability that becomes apparent at 20 degrees angle of attack. Therefore, the WTE curves are vertically translated to match the VLM curve at $\alpha = 15°$. The discontinuity that originates from this operation is resolved by interpolating the datapoints using the shape-preserving piecewise cubic interpolating polynomial function "pchip". This function makes use of splines, where each spline is a third-degree polynomial with specified derivatives at the interpolation points[†]. This results in a combined aerodynamic model, where the coefficients for angles of attack ranging between -5° up to 15° are obtained from the VLM model and the coefficients for angles of attack ranging between 15° up to 30° are obtained from the WTE model. Based on the aerodynamic model

[†]https://www.mathworks.com/help/matlab/ref/pchip.html#bvjbz1m-2

obtained from the combination of the VLM model and WTE model, it is concluded that the aerodynamic model does not contain any zero-lift drag (C_{D_0}), decreasing the fidelity of the model. Due to limited analysis on the zero-lift drag of a full scale model of the Flying-V it is decided to use the zero-lift drag from the Airbus A350-900 (the aircraft used as a reference for the design of the Flying-V) and add this to the aerodynamic model of the Flying-V. This results into a zero-lift drag of 0.027 during cruise and 0.057 during approach [23]. The combined aerodynamic model is shown in Fig. 5, where it is visible that the longitudinal unstable behaviour is captured by the combined aerodynamic model.

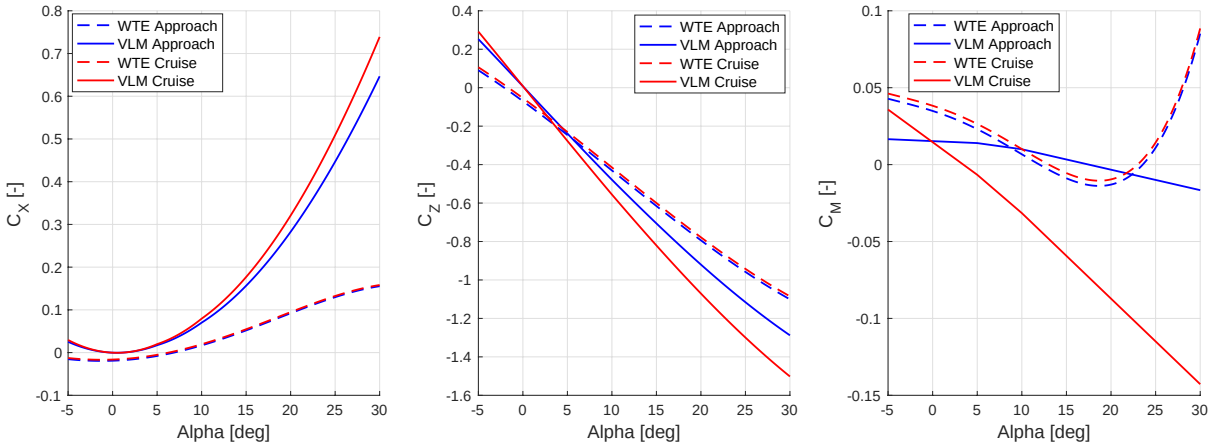

Fig. 4 Aerodynamic model curves from VLM and WTE for approach and cruise phase.

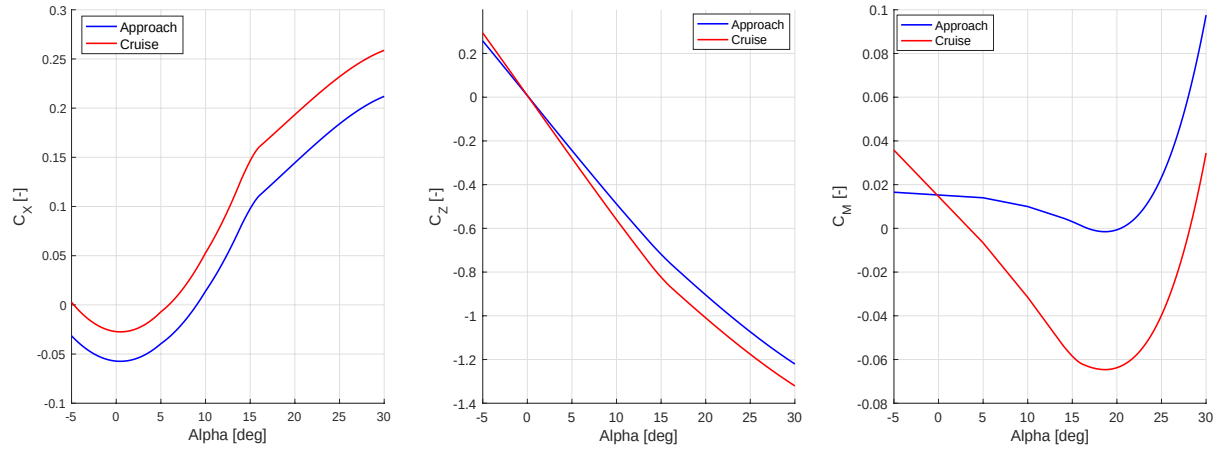

Fig. 5 Aerodynamic model obtained from combining VLM with WTE.

4. Verification and Validation

Before the simulation model to analyse the stability and handling qualities of the Flying-V can be used, it is first necessary to perform verification and validation on the model. This section first elaborates on the methodology used to verify the simulation model. After that, the validation methodology is discussed.

Simulation Model Verification

Before it is possible to analyse the simulation model results it is necessary to perform verification on the aerodynamic model and linearisation of the equations of motion. As mentioned in section II.A.2 it is necessary to linearise the equations of motion to determine specific parameters such as the damping ratio, natural frequency, and characteristic time constants to compare these with military standards.

For the verification of the aerodynamic model it is essential to analyse whether the aerodynamic model is implemented

correctly, and whether interpolation between datapoints is performed appropriately. The aerodynamic coefficients can be determined using linear interpolation between a set of data points arranged in a grid. Verification of the aerodynamic model is performed by two researchers using the same set of data points to obtain an aerodynamic model of the Flying-V. Consequently, the aerodynamic model results are compared for different inputs to obtain a range for which it can be guaranteed that a verified aerodynamic model is used.

To verify the results obtained from the linearised equations of motion, the response of the Flying-V to an input on the control surfaces is analysed and compared with the response of the nonlinear equations of motion. Small control surface inputs result in small deviations from the linearisation point. Therefore the response of the linearised simulation model is expected to be approximately equal to the response of the nonlinear simulation model. This comparative analysis is used to determine whether the linearisation is implemented correctly.

Simulation Model Validation

Validation of the simulation model of the Flying-V is ideally accomplished by comparison of accurately predicted aerodynamic responses of the aircraft from the simulation model with experimental tests [24]. However, using the flight test data from the maiden flight test[‡] for validation purposes is considered unreliable. This is because the flight test involves a small scale model, whereas the simulation model considers a full scale model. Therefore, it is necessary to apply Dynamic scaling to one of the models. This is however not possible due to a discrepancy between the mass distribution of the the full scale model and small scale model [13]. Besides that, Reynolds number effects will be present due to discrepancies between the airflow over the small scale model and full scale model [13]. Validation is therefore performed by first analysing the thrust setting during cruise. The thrust setting of an aircraft during cruise ranges between 20% and 30% of the maximum available thrust [§]. Besides that, it can be obtained that the thrust setting of the Airbus A350-900 is approximately 33.3% of the maximum available thrust[¶].

Furthermore, the simulation model results should be comparable with the results obtained from previous research [8, 11–13]. Therefore, the second validation analysis implies a comparative analysis between the eigenmodes obtained from the simulation model and previous research.

5. Assumptions and Limitations

During the design of the flight dynamic simulation model, several assumptions and therefore accompanying limitations have to be taken into account.

First of all, during the construction of the combined aerodynamic model, it is assumed that only the angle of attack makes a non-linear contribution to the force and moment coefficients. In reality, it is likely that other components (such as the control surfaces) also show nonlinear behaviour at high angles of attack. Therefore, it is expected that the fidelity of the contribution of these components to the forces and moments is limited.

Secondly, because the VLM model and WTE model both operate in different speed regimes due to the difference in aircraft size, it is necessary to apply Dynamic or Froude scaling. To apply this scaling method, the relative density factor and the relative moment of inertia of the small-scale model must be the same as in the full-scale aircraft [13]. This is not the case for the Flying-V and therefore results in inaccuracies of the combined aerodynamic model.

Moreover, because the VLM model is used as the baseline model, the combined aerodynamic model of the Flying-V does not contain frictional drag. It is not possible to obtain an accurate estimate of the frictional drag from the WTE model due to scaling. Frictional drag is therefore added to the combined aerodynamic model using data obtained from the Airbus A350-900.

In case the duration of the flight is short, the influence of the Earth's curvature and angular velocity is negligible. Therefore, the Earth can be assumed to be flat and the Coriolis acceleration and centripetal acceleration can be neglected. In case the period of the flight is large (in the order of hours), this introduces large errors that influence the accuracy of the simulation [25].

During the simulation zero wind and a perfect atmosphere is assumed that corresponds to the International Standard Atmosphere. Additional wind results in the fact that the kinematic velocity of the vehicle is different from the aerodynamic velocity. Wind conditions result in changing aerodynamic forces and moments acting on the aircraft, influencing the dynamic response of the vehicle.

Finally, because the Earth is not perfectly spherical with constant mass distribution, the gravity vector is not constant

[‡]https://www.tudelft.nl/en/2020/tu-delft/successful-maiden-flight-for-the-tu-delft-flying-v

[§]https://howthingsfly.si.edu/ask-an-explainer/i-assume-jet-engine-reaches-maximum-thrust-take-and-lift-cruising-elevation-and-red

[¶]https://www.airbus.com/aircraft/passenger-aircraft/a350xwb-family/a350-900.html

with respect to different locations on Earth. In reality, the gravity vector changes in direction and magnitude throughout the flight of the aircraft resulting in changing dynamic responses.

III. Results and Discussions

In this section, the results obtained from the flight dynamic simulation model are displayed and discussed. Section III.A shows the trim results. After that, the eigenmodes are discussed in section III.B. Furthermore, section III.C elaborates in the handling qualities results. Finally, the results from the verification and validation are shown in section III.D.

A. Trim

To assess the trimmability of the aircraft, for the cruise and approach phase, it is assumed that the aircraft is in a steady symmetric flight. Therefore the deflections of the rudders used for yaw control (δ_{CS3}) are set to zero. The trim algorithm aims at minimising the cost function shown in Eq. (4). In this equation, W_* represents the weight of each parameter of the cost function. The weights are determined iteratively and shown in Table 1. Besides that, $\dot{u}$, $\dot{w}$, and $\dot{q}$ are the time derivatives of the forward velocity component, vertical velocity component, and pitch rate respectively. Furthermore, V represents the airspeed, a represents the speed of sound, and γ is the flight path angle. As inputs, the trim function uses the forward velocity component (u), vertical velocity component (w), pitch angle (θ), elevon deflection angle of both the inboard and outboard elevons ($\delta_{CS1}/\delta_{CS2}$), and thrust setting ($T$). Consequently, the trim algorithm minimises the cost function using the MATLAB® function "fminsearch". This algorithm can be used to find the minimum of unconstrained multivariable functions using the Nelder-Mead simplex algorithm[‖]. The trim algorithm has three different stopping criteria. First of all, the trim algorithm stops in case the current function value differs by less than 10^{-9} from the previous function value. Besides that, the trim algorithm stops in case the current inputs differ from the previous inputs by less than 10^{-9}. In case these two criteria are not met, the trim algorithm stops in case the number of trim function evaluations exceeds 1,000,000.

$$J(\dot{u}, \dot{w}, \dot{q}, V, \gamma) = W_u \dot{u}^2 + W_w \dot{w}^2 + W_q \dot{q}^2 + W_V \left(\frac{V - V_{\text{ref}}}{a} \right)^2 + W_\gamma (\gamma - \gamma_{\text{ref}}) \tag{4}$$

Table 1 Weights for cost function.

Parameter	W_u	W_w	W_q	W_V	W_γ
Weight	100	1	100	100	1

The trim conditions for both the approach and cruise phase can be observed in Table 2. During approach, moving the centre of gravity forward leads to an increased angle of attack, control surface deflection, and thrust setting. Besides that, the flight path angle is equal to $\gamma = -3°$ as indicated by the requirements discussed in Section II.A.1. During cruise, moving the centre of gravity forward also leads to an increased angle of attack and control surface deflection, whereas the thrust setting remains similar.

The observed trends are due to the induced pitch down moment in case the centre of gravity is moved forward. To counteract this pitch down moment an increased (upwards) elevon deflection is required, which leads to a necessity to increase the lift force. This additional lift force can be obtained by increasing the angle of attack. It is expected that the thrust force mainly increases during approach due to a more significant angle of attack increase (3.4° during approach compared to 1.0° during cruise) and the larger air density during approach conditions. The results obtained from the trim conditions show the same trends as discussed in former research on the longitudinal flying qualities of blended-wing-body aircraft [26].

B. Modes Response

To analyse the eigenmodes of the aircraft, it is necessary to linearise the equations of motion such that the eigenvalues from a state-space system can be obtained. Therefore, nonlinear equations of motion are analytically linearised at the

[‖] https://www.mathworks.com/help/matlab/ref/fminsearch.html

Table 2 Trim Results

Flight Condition	Forward CG		Aft CG	
Approach (Ma = 0.2)	u	$64.1\frac{m}{s}$	u	$65.4\frac{m}{s}$
	w	$24.5\frac{m}{s}$	w	$20.7\frac{m}{s}$
	α	20.9°	α	17.5°
	θ	17.9°	θ	14.5°
	$\delta_{CS1}/\delta_{CS2}$	20.2°	$\delta_{CS1}/\delta_{CS2}$	3.9°
	T	$175642.8N$	T	$109867.0N$
Cruise (Ma = 0.85)	u	$248.8\frac{m}{s}$	u	$249.3\frac{m}{s}$
	w	$31.1\frac{m}{s}$	w	$26.8\frac{m}{s}$
	α	7.1°	α	6.1°
	θ	7.1°	θ	6.1°
	$\delta_{CS1}/\delta_{CS2}$	8.0°	$\delta_{CS1}/\delta_{CS2}$	2.6°
	T	$124199.7N$	T	$124377.6N$

trim conditions. In Section III.B.1, the eigenvalues obtained from the state-space system are discussed. Besides that, each eigenmode and the corresponding flying qualities are discussed below in Section III.B.2 - Section III.B.6.

1. Eigenvalue Analysis

After linearising the nonlinear equations of motion, it is possible to obtain the eigenvalues from the state-space system. The eigenvalues for each trim condition can be observed in Figure 6 and Figure 7. Furthermore, the natural frequency and damping ratio of each eigenmode for the different flight conditions are shown in Table 3.

First of all, the eigenvalues of the Flying-V during approach, shown in Figure 6, can be analysed. This figure shows how changing the centre of gravity location affects the location of the eigenvalues. Figure 6 shows that during approach, the short period mode and aperiodic roll mode are stable, whereas the phugoid mode, Dutch roll mode, and spiral mode are unstable. Furthermore, shifting the centre of gravity aft changes the location of the eigenvalues. First of all, for the oscillatory modes, the magnitude of the imaginary part of each eigenvalue decreases when moving the centre of gravity aft. Furthermore, the short period mode and aperiodic roll mode shift to a location closer to the imaginary axis. Besides that, the phugoid mode shifts further into the right half-plane. Finally, the Dutch roll mode and spiral mode (both located in the right half-plane) shift to a location closer to the imaginary axis.

Secondly, the eigenvalues of the Flying-V during cruise, shown in Figure 7, can be analysed. During cruise, the short period mode, phugoid mode, and aperiodic roll mode are stable, whereas the spiral mode is unstable. The Dutch roll mode is unstable at the forward centre of gravity location but stable at the aft centre of gravity location. During cruise the effect of shifting the centre of gravity aft is similar to approach. First of all, the magnitude of the imaginary part of each eigenvalue also decreases when moving the centre of gravity aft. Besides that, the short period mode, phugoid mode, and aperiodic roll mode shift to a location closer to the imaginary axis. Finally, the Dutch roll mode and spiral mode shift to the left. For the Dutch roll mode, this results in a stable mode during cruise at the aft centre of gravity location.

The results obtained from the eigenvalues are also shown in Table 3. This table shows the damping ratio and undamped natural frequency of each eigenmode. Moving the centre of gravity aft shows an increased short period damping ratio and decreased short period undamped natural frequency. Besides that, for the phugoid mode, shifting the centre of gravity aft results in a larger magnitude of the damping ratio in case the mode is unstable. The damping ratio decreases in case the mode is stable. The undamped natural frequency decreases when the centre of gravity is moved aft. The results obtained from Table 3 cohere with previous research on the handling qualities of a blended-wing-body aircraft [27]. Besides that, the results shown in Fig. 6, Fig. 7 show that the longitudinal stability deteriorates when moving the centre of gravity aft [27].

Looking at the Dutch roll mode, it can be observed that shifting the centre of gravity aft leads to larger magnitude of the damping ratio during approach. Besides that, during cruise, shifting the centre of gravity aft leads to a stable Dutch roll mode. Furthermore, the undamped natural frequency decreases when moving the centre of gravity aft. The

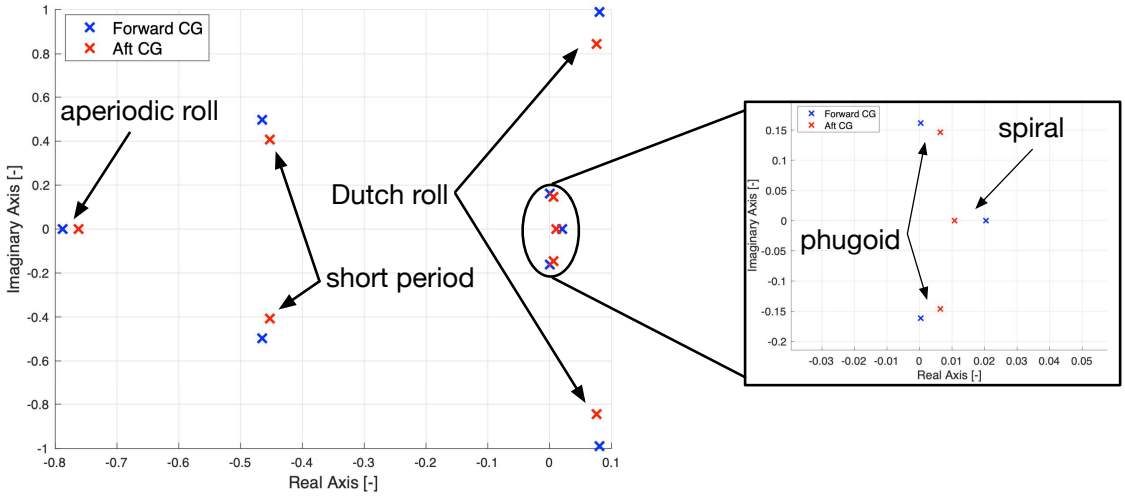

Fig. 6 Eigenvalues of the Flying-V during approach at forward and aft centre of gravity location.

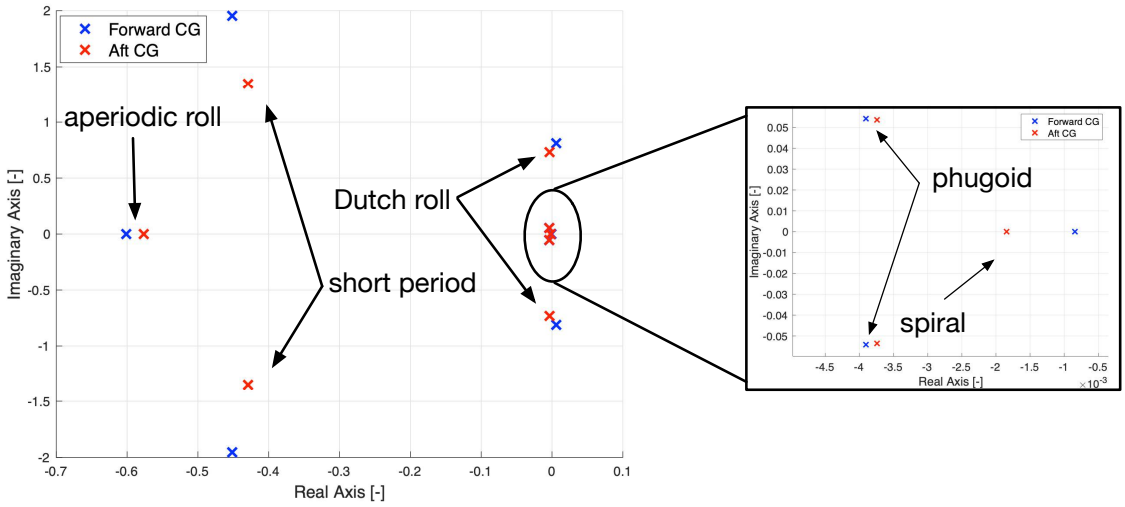

Fig. 7 Eigenvalues of the Flying-V during cruise at forward and aft centre of gravity location.

eigenvalues in Fig. 6 and Fig. 7 show that moving the centre of gravity aft moves the poles to the left. This is in contrast to former research that describes the deterioration of stability when moving the centre of gravity aft [27, 28].

Finally, the aperiodic roll mode and spiral mode are critically damped non-oscillatory modes and are therefore not considered in Table 3. However, looking at the aperiodic roll and spiral mode eigenvalues shown in 6 and Fig. 7, it can be observed that the magnitude eigenvalue increases when the centre of gravity is moved forward. This leads to a faster mode when moving the centre or gravity forward.

2. Short-period Mode

Section III.B.1 shows that the eigenvalues of the short-period mode consist of a negative real component during approach as well as cruise, meaning that this mode is stable. To analyse the flying quality level of the aircraft, it is necessary to determine the damping ratio of the short-period mode (ς_{sp}). The damping ratios and the requirements from military standards [18] can be observed in Table 4. It can be observed that the damping ratio during cruise is lower compared to approach. This decrease in damping ratio originates from the low air density at the cruise altitude of the

Table 3 Damping ratio and natural frequency for eigenmodes of the Flying-V.

Eigenmodes	Approach (Ma = 0.2)				Cruise (Ma = 0.85)			
	Forward		Aft		Forward		Aft	
	ς	ω	ς	ω	ς	ω	ς	ω
Short Period	0.683	0.681	0.744	0.609	0.225	2.01	0.303	1.41
Phugoid	$-2.31 \cdot 10^{-3}$	0.161	$-4.37 \cdot 10^{-2}$	0.146	$7.19 \cdot 10^{-2}$	$5.43 \cdot 10^{-2}$	$6.97 \cdot 10^{-2}$	$5.37 \cdot 10^{-2}$
Dutch Roll	$-8.14 \cdot 10^{-2}$	0.992	$-8.97 \cdot 10^{-2}$	0.848	$-7.38 \cdot 10^{-3}$	0.811	$4.68 \cdot 10^{-3}$	0.732
Aperiodic Roll	-	-	-	-	-	-	-	-
Spiral	-	-	-	-	-	-	-	-

Flying-V.

Table 4 shows that the short period mode of the Flying-V has Level 1 flying qualities at the approach condition and cruise condition at the aft centre of gravity location. Furthermore, the Flying-V shows Level 2 flying qualities at the forward centre of gravity location during cruise.

Table 4 Short-period flying qualities of the Flying-V.

	Approach (Ma = 0.2)		Cruise (Ma = 0.85)	
Forward CG	$\varsigma_{sp} = 6.83 \cdot 10^{-1}$		$\varsigma_{sp} = 2.25 \cdot 10^{-1}$	
Aft CG	$\varsigma_{sp} = 7.44 \cdot 10^{-1}$		$\varsigma_{sp} = 3.03 \cdot 10^{-1}$	
Short-period requirements	Level 1:	$0.5 < \varsigma_{sp} < 1.3$	Level 1:	$0.3 < \varsigma_{sp} < 2.0$
	Level 2:	$0.35 < \varsigma_{sp} < 2.0$	Level 2:	$0.2 < \varsigma_{sp} < 2.0$
	Level 3:	$\varsigma_{sp} > 0.25$	Level 3:	$\varsigma_{sp} > 0.1$

3. Phugoid Mode

Section III.B.1 shows that the real part of the eigenvalues of the phugoid mode are positive during approach and negative during cruise. This implies that the phugoid is unstable during approach. To analyse the flying quality level of the aircraft it is necessary to determine the damping ratio (ς_{ph}), and in case the phugoid is unstable, the period of the mode (T_{ph}). Using Table 5, these parameters can be compared with the military standards [18]. Table 5 shows that due to the small period of the unstable phugoid, the flying qualities during approach cannot be quantified by military standards. During cruise, the phugoid mode shows Level 1 flying qualities.

Table 5 Phugoid flying qualities of the Flying-V.

	Approach (Ma = 0.2)		Cruise (Ma = 0.85)	
Forward CG	Unstable but $T_{ph} = 39.0s$		$\varsigma_{ph} = 7.19 \cdot 10^{-2}$	
Aft CG	Unstable but $T_{ph} = 43.0s$		$\varsigma_{ph} = 6.97 \cdot 10^{-2}$	
Phugoid requirements	Level 1:	$\varsigma_{ph} > 0.04$	Level 1:	$\varsigma_{ph} > 0.04$
	Level 2:	$\varsigma_{ph} > 0$	Level 2:	$\varsigma_{ph} > 0$
	Level 3:	Unstable but $T_{ph} > 55s$	Level 3:	Unstable but $T_{ph} > 55s$

4. Dutch Roll Mode

In Section III.B.1, the eigenvalues from the Dutch roll mode show that the Dutch roll is unstable during approach, whereas the mode is stable when moving the centre of gravity aft during cruise. To analyse the flying quality level

of the aircraft it is necessary to determine damping ratio (ς_d) and undamped natural frequency of the motion (ω_d). The parameters obtained from military standards [18] and the simulation model can be observed in Table 6. This table shows that the flying quality level of an unstable Dutch roll mode cannot be quantified by military standards. Besides that, the Dutch roll mode during cruise at the aft centre of gravity location shows Level 3 flying qualities.

Table 6 Dutch roll flying qualities of the Flying-V.

	Approach (Ma = 0.2)			**Cruise (Ma = 0.85)**			
Forward CG	Unstable			Unstable			
Aft CG	Unstable			$\varsigma_d = 4.68 \cdot 10^{-3}$	$\varsigma_d\omega_d = 3.43 \cdot 10^{-3}$	$\omega_d = 0.732$	
Dutch roll requirements	Level 1:	$\varsigma_d > 0.08$	$\varsigma_d\omega_d > 0.10$	$\omega_d > 0.5$	Level 1:	$\varsigma_d > 0.08$	$\varsigma_d\omega_d > 0.15$	$\omega_d > 0.5$
	Level 2:	$\varsigma_d > 0.02$	$\varsigma_d\omega_d > 0.05$	$\omega_d > 0.5$	Level 2:	$\varsigma_d > 0.02$	$\varsigma_d\omega_d > 0.05$	$\omega_d > 0.5$
	Level 3:	$\varsigma_d > 0$	$\omega_d > 0.4$		Level 3:	$\varsigma_d > 0$	$\omega_d > 0.4$	

5. Aperiodic Roll Mode

The aperiodic roll for both the approach phase and the cruise phase is stable due to the negative real eigenvalue. To analyse the flying quality level of the aircraft, it is necessary to analyse the roll time constant (T_r) as can be observed in Table 7. The larger the roll time constant, the more time it takes to achieve a specific roll rate. Table 7 shows that the roll time constant is larger during the cruise condition and also increases when the centre of gravity is shifted aft. During approach the aperiodic roll shows Level 1 flying qualities. Besides that, during cruise the aperiodic roll shows Level 1 flying qualities at the forward centre of gravity location and Level 2 flying qualities at the aft centre of gravity location.

Table 7 Aperiodic roll flying qualities of the Flying-V.

	Approach (Ma = 0.2)	**Cruise (Ma = 0.85)**
Forward CG	$T_r = 1.26s$	$T_r = 1.32s$
Aft CG	$T_r = 1.32s$	$T_r = 1.71s$
Aperiodic roll requirements	Level 1: $T_r < 1.4s$	Level 1: $T_r < 1.4s$
	Level 2: $T_r < 3.0s$	Level 2: $T_r < 3.0s$
	Level 3: $T_r < 10.0s$	Level 3: $T_r < 10.0s$

6. Spiral Mode

The eigenvalues of the spiral mode show that the spiral is unstable during approach, but stable during cruise. A stable spiral mode automatically implies Level 1 flying qualities. The unstable behaviour of the spiral mode does not necessarily have to be critical as the flying quality level depends on the characteristic time constant for the spiral mode (T_s). The results are shown in Table 8. This table shows that for both the approach and cruise phase, the spiral mode has Level 1 flying qualities.

Table 8 Spiral mode flying qualities of the Flying-V.

	Approach (Ma = 0.2)	**Cruise (Ma = 0.85)**
Forward CG	$T_s = 42.6s$	Stable
Aft CG	$T_s = 79.4s$	Stable
Spiral requirements	Level 1: $T_s > 17.3s$	Level 1: $T_s > 28.9s$
	Level 2: $T_s > 11.5s$	Level 2: $T_s > 11.5s$
	Level 3: $T_s > 7.2s$	Level 3: $T_s > 7.2s$

C. Handling Qualities

For the handling quality analysis, the Control Anticipation Parameter is considered. The general equation for the Control Anticipation Parameter (CAP) can be observed in Eq. (5), where the parameter T_{θ_2} can be obtained from the second order transfer function shown in Eq. (6).

$$\text{CAP} = \frac{g\omega_{\text{sp}}^2 T_{\theta_2}}{V} \tag{5}$$

$$\frac{q(s)}{\delta_{\text{CS1}}(s)} = \frac{K_q(1 + T_{\theta_2} s)}{s^2 + 2\varsigma_{\text{sp}}\omega_{\text{sp}} + \omega_{\text{sp}}^2} \tag{6}$$

The state-space system obtained from the linearised Flying-V model does not result in a second-order transfer function. Namely, $\dot{q}$ depends on the states: u, w, p, q, and r. Therefore this state-space system is reduced to a system consisting of two states (w and q). The contribution of the other states is significantly smaller compared to these two states. Consequently, the Control Anticipation Parameters for the approach- and cruise phase at the different centre of gravity locations can be observed in Table 9. The results are graphically shown in Fig. 8. The values in Table 9 show that moving the centre of gravity aft results in a decreasing Control Anticipation Parameter. Besides that, the Control Anticipation parameter is lower during approach compared to cruise. This is mainly due to the low airspeed during approach, resulting in less effective control surfaces and a slower response of the Flying-V.

Table 9 Control Anticipation Parameter (CAP) Flying-V.

	Approach (Ma = 0.2)	**Cruise (Ma = 0.85)**
Forward CG	0.16	0.51
Aft CG	0.12	0.22

In Fig. 8 it can be observed that during approach, the Flying-V is on the border of Level 1 handling qualities at the forward centre of gravity and has Level 2 handling qualities at the aft centre of gravity. During cruise, the Flying-V has Level 1 handling qualities at the aft centre of gravity and has Level 2 handling qualities at the forward centre of gravity location. It is clear from the figures that moving the centre of gravity aft results in a lower CAP meaning that the response of the Flying-V becomes more sluggish when moving the centre of gravity aft, which may lead to oversteering. Similar behaviour is also apparent for other types of flying wings, where it is observed that the agility of the aircraft decreases in case the centre of gravity is moved aft [28].

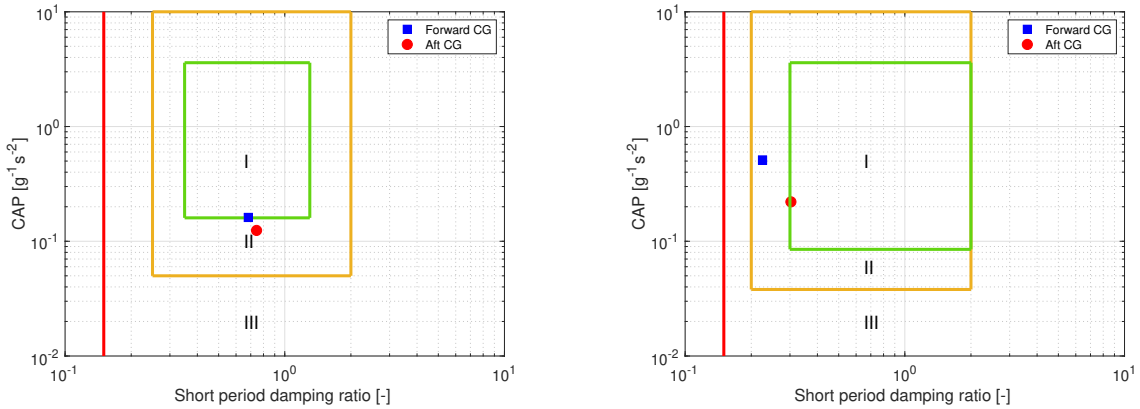

(a) CAP for approach phase.

(b) CAP for cruise phase.

Fig. 8 Control Anticipation Parameter (CAP) analysis.

D. Verification and Validation

In this section, the results obtained from the verification and validation procedure are discussed. First, section III.D.1 elaborates on the verification results. After that, the validation results are shown in section III.D.2.

1. Verification Results

The aerodynamic model is verified by analysing the aerodynamic model results generated by two different researchers using the same set of aerodynamic data points. Each aerodynamic coefficient is a function of the angle of attack, angle of sideslip, roll rate, pitch rate, yaw rate, and control surface deflections ($C_*(\alpha, \beta, p, q, r, \delta_{CS1}, \delta_{CS2}, \delta_{CS1})$). To verify the aerodynamic models, random inputs for each aerodynamic coefficient are determined. Consequently, the aerodynamic coefficients are compared. In case no error is obtained between the coefficients generated by the different researchers, the aerodynamic model is considered verified. This results in the operational range in which the aerodynamic model can be used as shown in Table 10.

Table 10 Verified Operational Range Aerodynamic Model Flying-V

Parameter	α	β	p,q,r	δ_{CS1}, δ_{CS2}, δ_{CS3}
Range	$[-5°; 30°]$	[-20 °; 20 °]	$[-10°/s; 10°/s]$	$[-25°; 25°]$

To verify the linearisation of the equations of motion, the time response of an input on the control surfaces of the nonlinear simulation model is compared with the time response of the linear simulation model. The time responses of an impulse input of 1° on the inboard elevons (pitch control), outboard elevons (roll control), and rudders (yaw control) can be observed in Fig. 9. The time responses show that the linear simulation model is able to approximate the response of the nonlinear simulation model for small deviations from the trim condition. It needs to be noted that large inputs on the control surfaces or large disturbances decrease the fidelity of the linear simulation model.

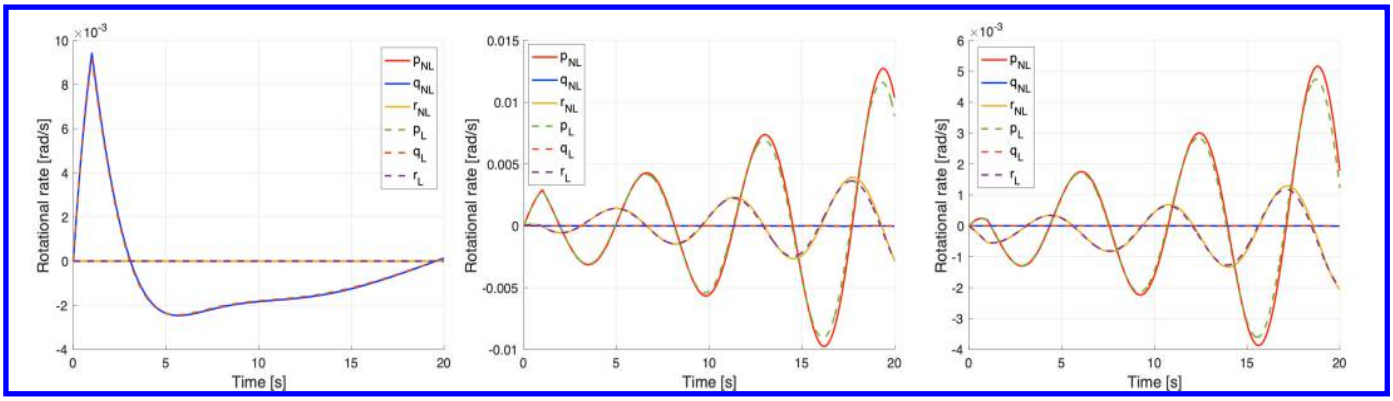

Fig. 9 Comparison between nonlinear simulation model and linearised simulation model.

2. Validation Results

To validate the simulation model of the Flying-V, it is first possible to analyse the thrust conditions during cruise at several centre of gravity locations. During cruise, the thrust setting is on average 124288.7 N. This corresponds to a thrust setting equal to 32.8% of the maximum available thrust. As discussed in section II.B.4, the thrust setting of an aircraft ranges in general between 20% and 30% of the maximum available thrust. Besides that, the thrust setting of the Airbus A350-900 is approximately 33.3%. It is therefore concluded that the thrust setting of the Flying-V coheres with literature, which validates the aerodynamic model used.

Furthermore, after obtaining the eigenvalue results, it is possible to compare the stability of different eigenmodes with literature to validate that the simulation model is able to capture the unstable Dutch roll mode and pitch break tendency for angles of attack larger than 20°. Previous research shows that the Dutch roll mode is unstable during approach conditions. Besides that, moving the centre of gravity forwards leads to an increased damping ratio and natural frequency of the mode [8]. The same conclusion can be drawn at the approach condition from Table 3. However, looking

at the cruise condition, it can be observed that moving the centre of gravity forwards leads to a decreased damping ratio. This is in contrast with previous research [8] and originates from the contribution of the aerodynamic coefficient C_{Y_p} in case the centre of gravity is moved forward. The sign and magnitude of this coefficient mainly depends on the size and location of the winglets of the Flying-V with respect to the centre of gravity location [29, 30]. The coefficient C_{Y_p} is negative for small angles of attack and becomes positive for larger angles of attack [31, 32]. Therefore, a forward shift of the centre of gravity leads to a decreased damping effect of the winglets and therefore results in opposite results of the Dutch roll damping compared to previous research.

Besides the Dutch roll mode, the simulation model has to capture the pitch break tendency for high angles of attack. Figure 5 shows that for angles of attack larger than 20°, C_{m_α} is larger than zero. This implies that for angles of attack larger than 20° pitch break occurs, meaning that the Flying-V becomes statically unstable [13]. This statically unstable behaviour is also discussed in previous research where the longitudinal flight characteristics of the Flying-V are investigated using wind tunnel experiments [11, 13].

IV. Conclusions

After analysing the aerodynamic models obtained from the Vortex Lattice Method (VLM) and wind tunnel experiments (WTE), it is concluded that one single aerodynamic model is not able to capture the unstable Dutch roll and unstable longitudinal behaviour obtained from previous research. Therefore, these aerodynamic models are combined. This combined aerodynamic model is integrated into the flight dynamic simulation model and is able to capture the unstable behaviour shown in previous research. However, the combined aerodynamic model is based on several critical assumptions, such as the assumptions that only the angle of attack makes a non-linear contribution to the force and moment coefficients, and that the relative density factor and the relative moment of inertia of the small-scale model are the same as in the full-scale aircraft, decreasing the fidelity of the model.

Furthermore, the short-period mode is stable and shows Level 1 flying qualities, except for cruise at the forward centre of gravity location where the short-period mode shows Level 2 flying qualities. The low damping ratio of the short period during cruise is due to the high design cruise altitude of the Flying-V. During approach the phugoid mode is unstable, whereas this mode shows Level 1 flying qualities during cruise. Besides that during approach conditions, the Flying-V is longitudinally statically unstable because C_{m_α} is larger than zero. This leads to perturbations in angle of attack being amplified instead of dampened.

Also, the Dutch roll mode is unstable during approach and shows Level 3 flying qualities during cruise at the aft centre of gravity location. The unstable Dutch roll mode indicates that the winglets of the Flying-V are not able to effectively dampen the Dutch roll mode. It is expected that increasing the size of the winglets improves the Dutch roll damping ratio. In case physical design changes are undesired, the Dutch roll damping can also be improved by designing an automatic flight control system that actively stabilises the Dutch roll.

From the control anticipation parameter (CAP) analysis it can be concluded that during approach, the CAP is rated Level 1 at the forward centre of gravity location. At the aft centre of gravity location, the CAP is rated Level 2, resulting in potential oversteering by the pilot. During cruise, the CAP is rated Level 2 at the forward centre of gravity, indicating that the damping ratio of the short period needs to be increased. Besides that, at the aft centre of gravity location, the CAP is rated Level 1 indicating that the pitch output of the Flying-V accurately follows the pitch input by a pilot.

V. Recommendations

With the goal to further improve research on modelling and handling quality assessment of the Flying-V aircraft, future work may include the set of items discussed in this section.

During this research, only the key stability and handling quality requirements for certification and qualification purposes are considered. It is therefore suggested to perform further research on additional requirements necessary for certification and qualification of the Flying-V.

Besides that, it is recommended to conduct further research on flight control systems that can be applied to the Flying-V to stabilise the unstable eigenmodes.

Finally, even though the aerodynamic model designed in this research is able to capture the undesired behaviour of the Flying-V obtained from previous research, several assumptions are made during the construction of the aerodynamic model. To increase the fidelity of the combined aerodynamic model, it is suggested to perform additional research on aerodynamic model identification of the Flying-V.

References

[1] Martinez-Val, R., Perez, E., Puertas, J., and Roa, J., "Optimization of Planform and Cruise Conditions of a Transport Flying Wing," *Proceedings of the Institution of Mechanical Engineers, Part G: Journal of Aerospace Engineering*, Vol. 224, No. 12, 2010, pp. 1243–1251. https://doi.org/10.1243/09544100JAERO812.

[2] Faggiano, F., Vos, R., Baan, M., and Van Dijk, R., "Aerodynamic Design of a Flying V Aircraft," *17th AIAA Aviation Technology, Integration, and Operations Conference*, 2017. https://doi.org/10.2514/6.2017-3589.

[3] Martinez-Val, R., "Flying Wings: A New Paradigm for Civil Aviation?" *Acta Polytechnica Vol. 47 No. 1/2007*, 2007. https://doi.org/10.14311/914.

[4] Okonkwo, P., and Smith, H., "Review of Evolving Trends in Blended Wing Body Aircraft Design," *Progress in Aerospace Sciences*, Vol. 82, 2016, pp. 1–23. https://doi.org/10.1016/j.paerosci.2015.12.002.

[5] Zhenli, C., Zhang, M., Yingchun, C., Weimin, S., Zhaoguang, T., Dong, L., and Zhang, B., "Assessment on Critical Technologies for Conceptual Design of Blended-Wing-Body Civil Aircraft," *Chinese Journal of Aeronautics*, Vol. 32, No. 8, 2019, pp. 1797–1827. https://doi.org/10.1016/j.cja.2019.06.006.

[6] Liebeck, R. H., "Design of the blended wing body subsonic transport," *Journal of aircraft*, Vol. 41, No. 1, 2004, pp. 10–25. https://doi.org/10.2514/1.9084.

[7] Benad, J., "The Flying V, A New Aircraft Configuration for Commercial Passenger Transport," *Deutscher Luft- und Raumfahrtkongress*, 2015. https://doi.org/10.25967/370094.

[8] Cappuyns, T., "Handling Qualities of a Flying V Configuration," http://resolver.tudelft.nl/uuid:69b56494-0731-487a-8e57-cec397452002, 2019.

[9] Humphreys-Jennings, C., Lappas, I., and Sovar, D. M., "Conceptual Design, Flying, and Handling Qualities Assessment of a Blended Wing Body (BWB) Aircraft by Using an Engineering Flight Simulator," *Aerospace*, Vol. 7, No. 5, 2020, p. 51. https://doi.org/10.3390/aerospace7050051.

[10] Ammar, S., Legros, C., and Trépanier, J.-Y., "Conceptual Design, Performance and Stability Analysis of a 200 Passengers Blended Wing Body Aircraft," *Aerospace Science and Technology*, Vol. 71, 2017, pp. 325–336. https://doi.org/10.1016/j.ast.2017.09.037.

[11] Palermo, M., and Vos, R., "Experimental Aerodynamic Analysis of a 4.6%-Scale Flying-V Subsonic Transport," *AIAA Scitech 2020 Forum*, 2020, p. 2228. https://doi.org/10.2514/6.2020-2228.

[12] Viet, R., "Analysis of the Flight Characteristics of a Highly Swept Cranked Flying Wing by Means of an Experimental Test," http://resolver.tudelft.nl/uuid:90de4d9e-70ae-4efc-bd0a-7426a0a669c3, 2019.

[13] Garcia, A.R., "Aerodynamic Model Identification of the Flying V using Wind Tunnel Data," http://resolver.tudelft.nl/uuid:79e01f29-1789-4501-8556-ca2bcf06f3ab, 2019.

[14] CS-25, "Easy Access Rules for Large Aeroplanes (CS-25)," , 2018. Accessed: 23-02-2021.

[15] Perez, R. E., Liu, H. H., and Behdinan, K., "Multidisciplinary Optimization Framework for Control-Configuration Integration in Aircraft Conceptual Design," *Journal of Aircraft*, Vol. 43, No. 6, 2006, pp. 1937–1948. https://doi.org/10.2514/1.22263.

[16] Wahler, N.F.M., "The Impact of Control Allocation on Optimal Control Surface Positioning and Sizing," http://resolver.tudelft.nl/uuid:5e9baf63-8a8f-4c1b-98cd-5aa993938027, 2021.

[17] Cook, M.V., *Flight Dynamics Principles: A Linear Systems Approach to Aircraft Stability and Control*, Butterworth-Heinemann, 2012.

[18] Anonymous, "Military Specifications, Flying Qualities of Piloted Aircraft MIL-F-8785C," , 1980.

[19] Grotens, R., "Nonlinear Flight Control Fault Tolerant Control with Sliding Modes and Control Allocation," http://resolver.tudelft.nl/uuid:29ddf25f-bcc3-47f3-9c26-53da9b6d9301, 2010.

[20] Sieberling, S et al., "Robust Flight Control using Incremental Nonlinear Dynamic Inversion and Angular Acceleration Prediction," *Journal of Guidance, Control, and Dynamics*, Vol. 33, No. 6, 2010, pp. 1732–1742.

[21] Lambert, T., Abdul Razak, N., and Dimitriadis, G., "Vortex Lattice Simulations of Attached and Separated Flows around Flapping Wings," *Aerospace*, Vol. 4, No. 2, 2017, p. 22. https://doi.org/10.3390/aerospace4020022.

[22] Ananda, G. K., Vahora, M., Dantsker, O. D., and Selig, M. S., "Design Methodology for a Dynamically-Scaled General Aviation Aircraft," *35th AIAA Applied Aerodynamics Conference*, 2017, p. 4077. https://doi.org/10.2514/6.2017-4077.

[23] Sun, J. et al., "Aircraft Drag Polar Estimation Based on a Stochastic Hierarchical Model," *8th International Conference on Research in Air Transportation*, 2018.

[24] Murphy, P. et al., "Validation of Methodology for Estimating Aircraft Unsteady Aerodynamic Parameters from Dynamic Wind Tunnel Tests," *AIAA Atmospheric Flight Mechanics Conference and Exhibit*, 2003, p. 5397.

[25] Mulder, J.A., Van Staveren, W.H.J.J., Van der Vaart, J.C., De Weerdt, E., De Visser, C.C., In 't Veld, A.C. and Mooij, E., *Flight Dynamics*, TU Delft, 2013.

[26] Cook, M., and De Castro, H., "The Longitudinal Flying Qualities of a Blended-Wing-Body Civil Transport Aircraft," *The Aeronautical Journal*, Vol. 108, No. 1080, 2004, pp. 75–84.

[27] De Castro, H. V., "Flying and Handling Qualities of a Fly-By-Wire Blended-Wing-Body Civil Transport Aircraft," Ph.D. thesis, Cranfield University, 2003.

[28] Hasan, Y. J., Schwithal, J., Pfeiffer, T., Liersch, C. M., and Looye, G., *Handling Qualities Assessment of a Blended Wing Body Configuration under Uncertainty Considerations*, Deutsche Gesellschaft für Luft-und Raumfahrt-Lilienthal-Oberth eV, 2018.

[29] Finck, R., "USAF (United States Air Force) Stability and Control DATCOM (Data Compendium)," Tech. rep., MC Donnell Aircraft Co St. Louis Mo, 1978.

[30] Toll, T. A., and Queijo, M. J., "Approximate Relations and Charts for Low-Speed Stability Derivatives of Swept Wings," 1948.

[31] Anton, N., Botez, R., and Popescu, D., "New Methodologies for Aircraft Stability Derivatives Determination From its Geometrical Data," 2009, p. 6046.

[32] Ahmad, M., Hussain, Z. L., Shah, S. I. A., and Shams, T. A., "Estimation of Stability Parameters for Wide Body Aircraft Using Computational Techniques," *Applied Sciences*, Vol. 11, No. 5, 2021, p. 2087.